Article

Cancer Cell

Inhibition of Spleen Tyrosine Kinase Potentiates Paclitaxel-Induced Cytotoxicity in Ovarian Cancer Cells by Stabilizing Microtubules

Graphical Abstract

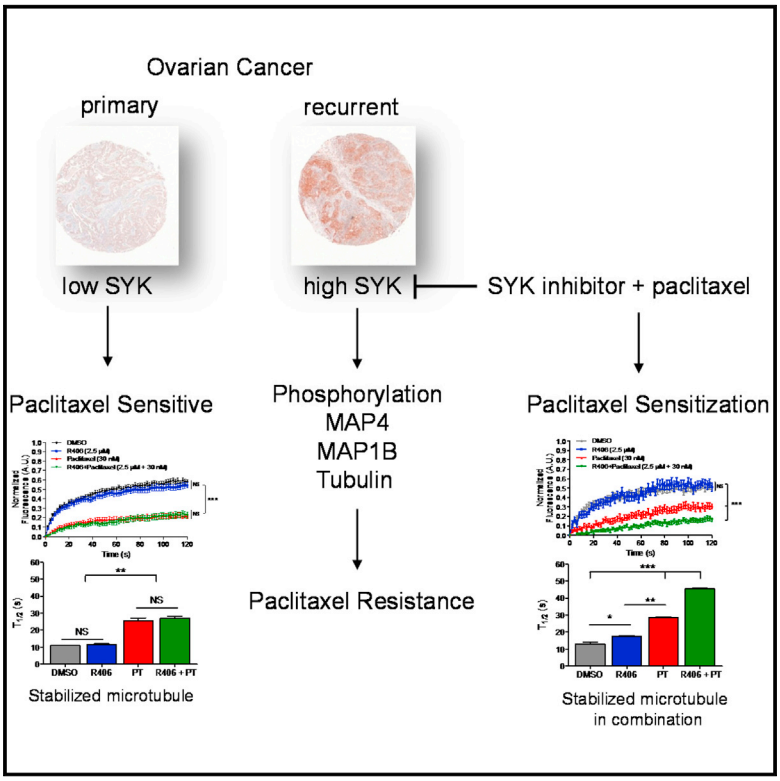

Highlights

- SYK is overexpressed in recurrent post-chemotherapy ovarian cancers
- Inhibition of SYK synergistically enhances sensitivity to paclitaxel in tumor cells
- SYK inhibition stabilizes microtubule in the presence of paclitaxel
- Tubulin and MAPs are SYK substrates that may contribute to paclitaxel resistance

Authors

Yu Yu, Stephanie Gaillard, Jude M. Phillip, ..., Ben Davidson, Tian-Li Wang, Ie-Ming Shih

Correspondence

tlw@jhmi.edu (T.-L.W.), ishih@jhmi.edu (I.-M.S.)

In Brief

Yu et al. show that ovarian cancer cells surviving paclitaxel treatment have higher levels of activated spleen tyrosine kinase (SYK). Importantly, inhibition of SYK sensitizes ovarian cancer cells to paclitaxel treatment via enhancing microtubule stability.

Yu et al., 2015, Cancer Cell *28*, 82–96
July 13, 2015
http://dx.doi.org/10.1016/j.ccell.2015.05.009

CellPress

Cancer Cell
Article

Inhibition of Spleen Tyrosine Kinase Potentiates Paclitaxel-Induced Cytotoxicity in Ovarian Cancer Cells by Stabilizing Microtubules

Yu Yu,[1] Stephanie Gaillard,[1,9] Jude M. Phillip,[3] Tai-Chung Huang,[2] Sneha M. Pinto,[2] Nayara G. Tessarollo,[1,4] Zhen Zhang,[1] Akhilesh Pandey,[1,2] Denis Wirtz,[1,3] Ayse Ayhan,[1,5] Ben Davidson,[6,7] Tian-Li Wang,[1,*] and Ie-Ming Shih[1,8,*]

[1]Department of Pathology and Sidney Kimmel Comprehensive Cancer Center, Johns Hopkins Medical Institutions, Baltimore, MD 21205, USA
[2]Department of Biological Chemistry and Oncology, Johns Hopkins Medical Institutions, Baltimore, MD 21205, USA
[3]Department of Chemical and Biomolecular Engineering, Physical Sciences-Oncology Center, and Institute for NanoBioTechology, Johns Hopkins University, Baltimore, MD 21218, USA
[4]Biotechnology Program/Renorbio, Health Science Center, Federal University of Espirito Santo, Vitória 29075-910, Brazil
[5]Department of Pathology, Seirei Mikatahara Hospital and Hamamatsu University School of Medicine, Hamamatsu 431-3192, Japan
[6]Department of Pathology, Oslo University Hospital, Norwegian Radium Hospital, 0310 Oslo, Norway
[7]Institute of Clinical Medicine, Faculty of Medicine, University of Oslo, 0316 Oslo, Norway
[8]Department of Gynecology and Obstetrics, Johns Hopkins Medical Institutions, Baltimore, MD 21287, USA
[9]Present address: Department of Oncology, Duke Medical Center, Durham, NC 27710, USA
*Correspondence: tlw@jhmi.edu (T.-L.W.), ishih@jhmi.edu (I.-M.S.)
http://dx.doi.org/10.1016/j.ccell.2015.05.009

SUMMARY

Resistance to chemotherapy represents a major obstacle for long-term remission, and effective strategies to overcome drug resistance would have significant clinical impact. We report that recurrent ovarian carcinomas after paclitaxel/carboplatin treatment have higher levels of spleen tyrosine kinase (SYK) and phospho-SYK. In vitro, paclitaxel-resistant cells expressed higher SYK, and the ratio of phospho-SYK/SYK positively associated with paclitaxel resistance in ovarian cancer cells. Inactivation of SYK by inhibitors or gene knockdown sensitized paclitaxel cytotoxicity in vitro and in vivo. Analysis of the phosphotyrosine proteome in paclitaxel-resistant tumor cells revealed that SYK phosphorylates tubulins and microtubule-associated proteins. Inhibition of SYK enhanced microtubule stability in paclitaxel-resistant tumor cells that were otherwise insensitive. Thus, targeting SYK pathway is a promising strategy to enhance paclitaxel response.

INTRODUCTION

Development of resistance to chemotherapeutic agents is a prevalent and challenging problem in managing cancer (Holohan et al., 2013). The high morbidity and mortality associated with many types of human cancer are attributed to the emergence of tumor cells that are refractory to cytotoxic chemotherapy and clonally develop into recurrent tumors. Although The Cancer Genome Atlas and several other genome-wide studies have revealed the molecular landscapes of cancer, these studies mainly focus on primary tumors (Vogelstein et al., 2013). It is critical, however, to study recurrent tumors and elucidate the molecular etiology of drug resistance. Toward this goal, we previously studied ovarian high-grade serous carcinoma (HGSC) to identify genes and the pathways they controlled in the development of recurrent disease. HGSC is the most common and lethal type of ovarian cancer (Cho and Shih, 2009); most patients are diagnosed with advanced-stage disease and require first-line

Significance

There is an unmet need to introduce more effective drugs to enhance therapeutic effects of current chemotherapeutic agents. Here, we demonstrated that inactivating spleen tyrosine kinase (SYK) using small compound inhibitors sensitized cells to the cytotoxic effects of paclitaxel, overcoming paclitaxel resistance. We found that SYK inhibitors stabilized microtubules through dephosphorylation of microtubule and microtubule-associated proteins, a mechanism that is distinct from paclitaxel. As a result, SYK inhibitor and paclitaxel formed a synergistic cytotoxic effect in tumor cells, especially in those that were paclitaxel-resistant. Our results provide critical pre-clinical evidence proposing the use of SYK inhibitors in combination with paclitaxel in cancer patients, and warrant future clinical studies to assess the clinical benefit of such combined therapy.

therapy, which involves cytoreductive surgery followed by combined carboplatin and paclitaxel chemotherapy. Although HGSC generally responds to this standard chemotherapy at the beginning of its course, relapse usually occurs and requires further therapy including the weekly paclitaxel regimen. Unfortunately, only a small percentage (10%–15%) of patients with advanced disease achieve long-term remission.

In a previous study, we compared proteomes between primary and recurrent post-chemotherapy HGSC tissues from the same patients (Jinawath et al., 2010). Among the preferentially expressed proteins identified in recurrent HGSCs, the non-receptor tyrosine kinase, spleen tyrosine kinase (SYK), was of interest because more than half of the recurrent tumors expressed higher levels of SYK than did the primary tumors (Jinawath et al., 2010). This is significant because small molecule inhibitors that target SYK, such as fostamatinib (R788), are available for preclinical testing and for future clinical trials in patients with ovarian cancer (Ruzza et al., 2009).

Originally isolated from bovine thymus (Zioncheck et al., 1986) and later identified in activated B lymphocytes (Hutchcroft et al., 1991; Zioncheck et al., 1988), SYK regulates adaptive immune receptor signaling, cell proliferation, differentiation, and survival. SYK has been reported as a candidate oncogene in B cell leukemia and lymphomas, gastric carcinoma, and head and neck cancer (Buchner et al., 2009; Feldman et al., 2008; Luangdilok et al., 2007; Mócsai et al., 2010; Nakashima et al., 2006). SYK expression has an anti-apoptotic effect on B-lymphoma cell lines through phosphorylation of nucleolin, which stabilizes the mRNA of anti-apoptotic Bcl-x(L) (Wang et al., 2014). Paradoxically, SYK expression may block tumor progression in breast cancer because loss of its expression is associated with poor prognosis and tumor metastasis (Coopman et al., 2000). The evidence thus suggests that SYK can either negatively or positively regulate tumor progression, depending on the biological context and tissue lineage (Geahlen, 2014).

The purpose of this study is to determine how SYK contributes to chemoresistance in ovarian cancers and to establish a biological foundation for introducing SYK inhibitors to potentiate the anti-tumor effects of chemotherapeutic drugs. We also seek to identify candidate SYK substrates involved in drug resistance, and the results should have translational implications to improve chemotherapy and clinical outcomes in patients with cancer.

RESULTS

Recurrent Ovarian Tumors Express Higher Levels of SYK and Phosphorylated SYK

To compare the expression levels of SYK in paired recurrent post-chemotherapy ovarian HGSC and their primary untreated tumors, we performed immunohistochemistry using two antibodies, one specific for SYK and the other specific for its active (autophosphorylated) form, p-SYK (Y525/526). Using the H score to semi-quantify immunoreactivity, we found that H scores for SYK were higher in the recurrent ovarian HGSC specimens than in the primary counterparts (Figure 1A), and H scores for active p-SYK (Y525/526) were higher in recurrent tumors than in primary tumors (Figure 1B). Likewise, H scores of total SYK or p-SYK positively correlated to each other (Figure 1C). Representative staining for p-SYK in a pair of matched primary and recurrent ovarian HGSC is shown in Figure 1D. Aside from HGSC, upregulated SYK expression was also observed in four of six cases of recurrent post-chemotherapy ovarian clear cell carcinomas as compared to matched primary tumors (Figure S1A). We further examined SYK expression using immunohistochemistry in 214 serous ovarian carcinoma effusions (Table S1; see the Supplemental Experimental Procedures for the cohort information) and observed an association ($p = 0.005$) between higher SYK staining intensity and less favorable chemoresponse to paclitaxel/platinum-based combination therapy. These data support that SYK upregulation is associated with chemoresistance.

Association between Paclitaxel Resistance and SYK

Because the recurrent HGSC tissues were obtained from patients who were previously treated with carboplatin and paclitaxel combination therapy, we sought to determine if SYK overexpression was related to resistance of carboplatin or paclitaxel. We analyzed two ovarian cancer cell lines, SKOV3 and MPSC1, from which carboplatin resistant and paclitaxel-resistant (TR) clones were previously established (Jinawath et al., 2009, 2010). We found that paclitaxel-resistant SKOV3TR and MPSC1TR expressed higher levels of SYK and p-SYK (Y525/526) than the parental cells (Figures 1E and 1F), suggesting that SYK upregulation was related to biological resistance to paclitaxel and is unlikely due to acute induction by paclitaxel in naive cells (Figure S1B).

To examine if there is an association between SYK activity and response to paclitaxel, we analyzed a panel of 25 primary ovarian cancer cell cultures and cell lines expressing different levels of SYK by immunoblotting (Figure S1C). The degree of paclitaxel sensitivity in these cells was determined by their half-maximal inhibitory concentration (IC_{50}) values. A significant positive correlation was observed between p-SYK/SYK ratios and the IC_{50} of paclitaxel but not carboplatin (Figure 1G), suggesting that active SYK is an important determinant of paclitaxel resistance.

Inactivation of SYK Suppresses Cell Growth in Ovarian Cancer Cells

To determine if SYK can be a therapeutic target in ovarian cancer, we inactivated SYK using shRNAs or small molecule inhibitors. We found that SYK knockdown, as compared to control knockdown, significantly reduced cell numbers in naive (parental) SKOV3 and MPSC1 as well as in their corresponding paclitaxel-resistant clones, although the SYK knockdown achieved in resistant cells was not as pronounced as in the naive cells (Figure 2A). Next, we treated SKOV3 cells with the SYK inhibitor R406 (the active metabolite of fostamatinib) and observed that R406 suppressed SYK autophosphorylation at Y525/526 and Y352, which was considered an indicator for SYK activation (Figure 2B) and resulted in concentration-dependent inhibition of SYK activity as measured by reduction of p-SYK (Y525/526) (Figure S2A). We further observed that R406 inhibited proliferation in a dose-dependent manner in SKOV3, SKOV3TR, MPSC1, and MPSC1TR cells (Figure 2C).

Next, we determined the sensitivity to R406 in a panel of cell lines with various levels of endogenous SYK expression (Figure 2D). Based on western blot analysis, we separated cell lines into SYK-expressing and undetectable groups and observed

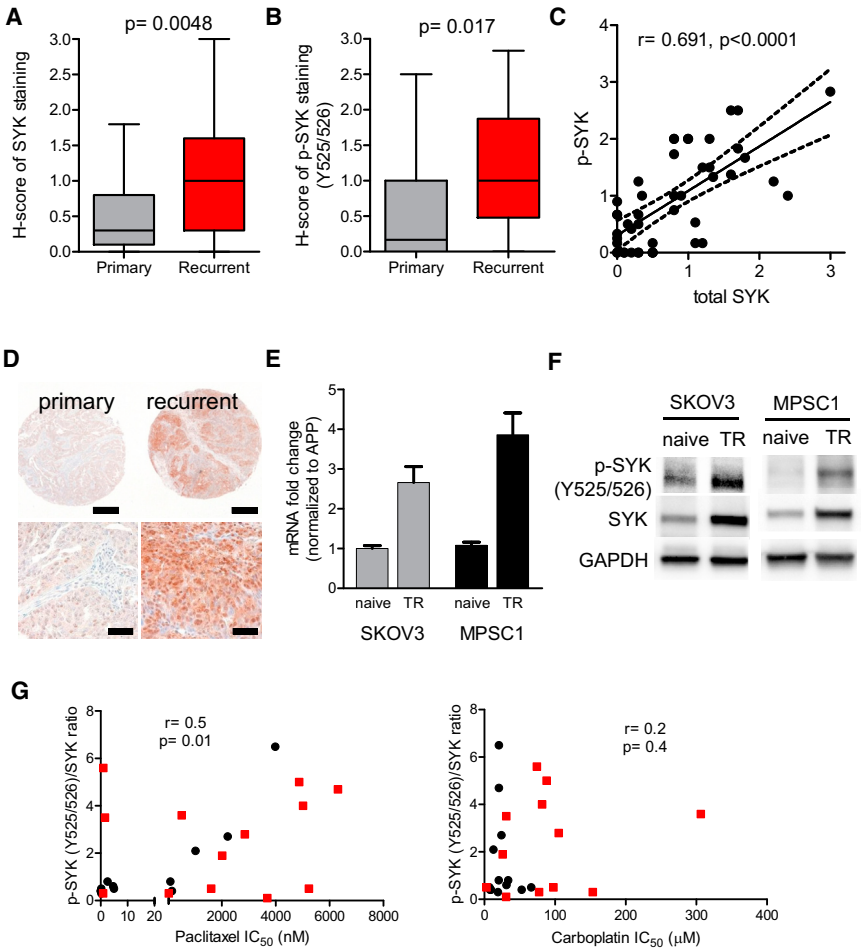

Figure 1. Expression of SYK and Phosphorylated SYK in Primary and Recurrent Ovarian Cancers

(A and B) Immunohistochemistry shows levels of SYK (A) and phospho-SYK (p-SYK, Y525/526) (B) in recurrent ovarian HGSCs compared to primary untreated specimens from the same patients based on paired two-tailed t test (n = 23 pairs). H score is used to semi-quantify the expression levels. The bottom and top of the boxplots represent the first and third quartiles, the band inside the box is the median, and the lines above and below the box indicate the maximum and minimum of all of the data.

(C) Correlation of H scores between total SYK and p-SYK levels.

(D) Representative images of p-SYK staining from matched primary and recurrent tumors. Scale bars represent approximately 400 μm (top) and 40 μm (bottom).

(E and F) mRNA (E) and protein (F) expression of SYK and p-SYK in SKOV3 and MPSC1 naive and paclitaxel-resistant (TR) cells.

(G) Pearson correlation analysis between p-SYK/SYK ratio and paclitaxel or carboplatin sensitivity (as determined by IC_{50}) in a panel of primary ovarian cancer cell cultures (red) and cell lines (black). Results are shown as ± SEM. See also Figure S1 and Table S1.

significantly greater sensitivity to R406 (lower IC_{50} values) in SYK-expressing cell lines than in cell lines with undetectable levels of SYK expression (Figure 2E). Calculation of Spearman's rank correlation coefficient demonstrated a negative correlation between SYK expression and the IC_{50} values for R406 (Figure 2F). Similarly, an inverse correlation between p-SYK (Y525/526) expression levels and the IC_{50} values of R406 was observed in these cell lines (Figure S2B).

SYK Inhibitors Enhance Paclitaxel Sensitivity

We then tested the effect of combining R406 with chemotherapeutic agents including paclitaxel, docetaxel, carboplatin, 5-fluorouracil, doxorubicin, mitomycin C, and methotrexate. Based on the drug combination index, we found that microtubule-targeting agents, including paclitaxel and docetaxel, had a synergistic effect with R406, whereas other drugs, including carboplatin, produced no such effect (Figures 3A and S3A). The ability of SYK inhibitor to enhance paclitaxel cytotoxicity was dose dependent because higher R406 concentrations were associated with a greater inhibitory effect (Figure 3B). Enhancement of paclitaxel sensitivity was also observed by SYK knockdown using shRNAs (Figures S3B and S3C) and siRNAs (Figures S3D and S3E). In other primary ovarian tumor cell cultures and ovarian cancer cell lines that exhibited high intrinsic resistance to paclitaxel ($IC_{50} \geq 5$ nM), the combination of paclitaxel and SYK inhibitors was also synergistic (Figure 3D; Figure S3F). The use of other SYK inhibitors including P505-15/PRT062607 and GS-9973 (Figure 3C) (Currie et al., 2014; Hoellenriegel et al., 2012) produced a similar result. In cell lines with high levels of SYK, including OVCAR3 and OVCA429, the same synergistic effect was also observed (Figure S3F). These data suggest that the effect observed from R406 was unlikely due to non-specific pan-kinase inhibition.

The effect of R406 on paclitaxel-induced cytotoxicity was further compared between paclitaxel-resistant and -naive cells. We found that treatment with SYK inhibitors resulted in a prominent shift of the paclitaxel IC_{50}s in both SKOV3TR and MPSC1TR cells compared to parental SKOV3 and MPSC1 cells. Specifically, the ratio of paclitaxel IC_{50} in untreated to R406 treated SKOV3 cells was 2.5, whereas in SKOV3TR it was 236 (Figure 3E). The ratio of paclitaxel IC_{50} for MPSC1 cells in untreated cells to R406 treated cells was 8, whereas in MPSC1TR it was 12,429 (Figure 3F), suggesting that paclitaxel-resistant cells were much more sensitive to the combined SYK inhibitor and paclitaxel treatment than their parental counterparts. The other SYK inhibitors also showed synergistic relationship with paclitaxel in the resistant SKOV3TR and MPSC1TR cells (Figure S3F).

Combination of R406 and Paclitaxel Induces G2/M Arrest and Enhances Apoptosis

Because paclitaxel targets microtubules, the above results suggested that SYK may also regulate microtubule function, which is essential for mitosis. Therefore, we quantified cell cycle

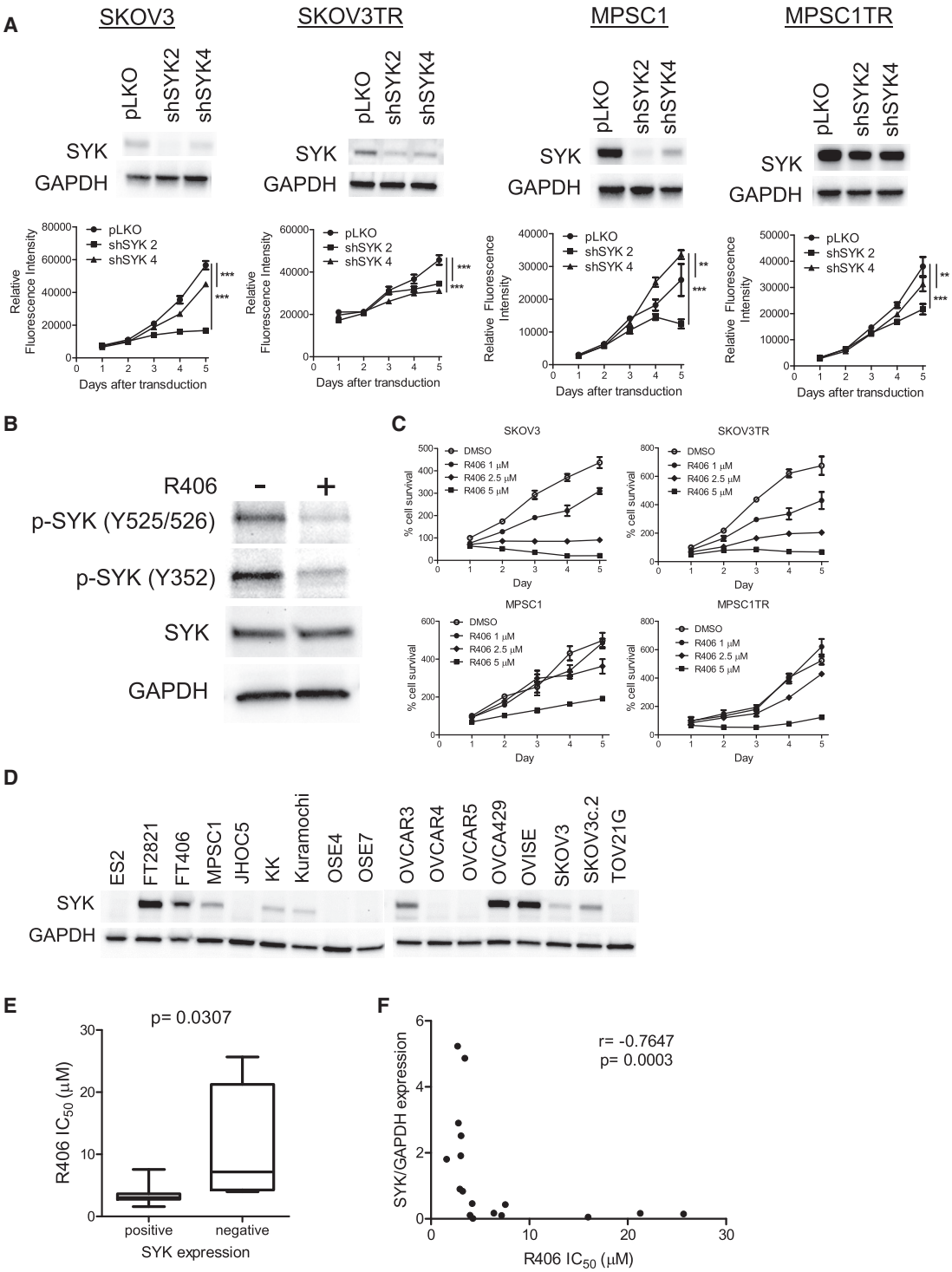

Figure 2. SYK Knockdown or SYK Inhibitor Reduces Ovarian Cancer Cell Growth

(**A**) Immunoblot shows SYK knockdown efficiency 48 hr after transduction with lentivirus expressing SYK shRNAs as compared to control shRNA (pLKO.1). GAPDH is the loading control. Cell numbers are determined daily. **p < 0.01; ***p < 0.001 as determined by two-way ANOVA with Bonferroni posttests.

(B) Western blot analysis of SKOV3 tumor spheroids 48 hr after R406 (2.5 μM) treatment.

(C) The effect of R406 on cellular proliferation.

(D) Immunoblot shows SYK expression levels in indicated cell lines.

(E) R406 IC_{50} in cells with or without detectable SYK expression (paired t test). The bottom and top of the boxplots represent the first and third quartiles, the band inside the box is the median, and the lines above and below the box indicate the maximum and minimum of all of the data.

(F) Spearman correlation analysis between SYK expression levels and R406 IC_{50} values. Results are shown as ± SEM. See also Figure S2.

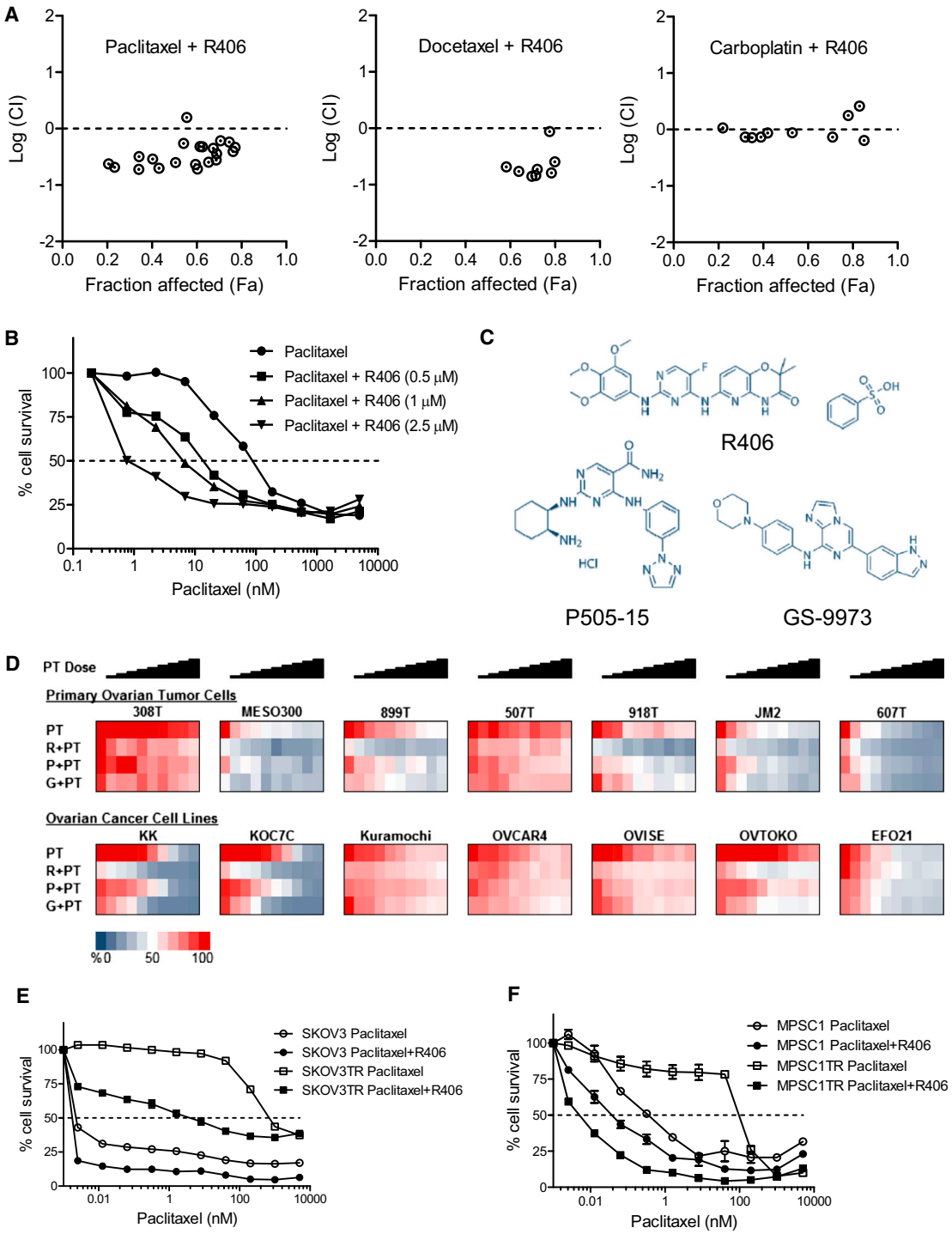

Figure 3. Combination of SYK Inhibitor and Paclitaxel Produces a Synergistic Cytotoxicity

(A) Logarithmic combination index plot of R406 (2.5 μM) is generated in combination with paclitaxel, docetaxel or carboplatin in paclitaxel-resistant SKOV3TR cells.

(B) Cell viability assay in SKOV3TR cells treated with paclitaxel and R406 at indicated concentrations.

(C) Structures of SYK inhibitors used in the study.

(D) Heatmaps of cell viability after treatment with paclitaxel or combination of SYK inhibitor and paclitaxel in primary ovarian cancer cells and cell lines. PT, paclitaxel; R, R406; P, P505-15/PRT062607; G, GS-9973. Blue to red: cell viability from low to high.

(E and F) Dose-response curves showing the effect of addition of R406 to paclitaxel in paclitaxel-resistant cells as compared to naive SKOV3 cells (E) or MPSC1 cells (F). Results are shown as ± SEM. See also Figure S3.

distribution in cells treated with R406, paclitaxel, or their combination. It is known that paclitaxel induces microtubule stabilization and leads to mitotic block in the late G2/M phase of the cell cycle. Based on high-throughput imaging analysis of in vitro cell cultures using Hoechst 33342 staining of DNA, we were able to confirm that paclitaxel increased the fraction of SKOV3 cells at the G2/M phase 8 hr, 12 hr, or 16 hr after treatment (Figures S3G and S3H). In contrast, SKOV3TR cells did not respond to paclitaxel treatment alone, but arrested in G2/M phase only when the cells were co-treated with R406. In addition, the levels of apoptosis markers, cleaved PARP, and caspase 7 (Figure S3I) and annexin V staining (Figure S3J) increased when cells were co-treated with R406 and paclitaxel compared to the cells treated with vehicle control, R406, or paclitaxel only.

Combination of R406 and Paclitaxel Inhibits Tumor Growth in Naive and Paclitaxel-Resistant Ovarian Tumor Xenograft

Two mouse models were used to assess the anti-tumor effect of R406, paclitaxel, and the combination. In the first model, SKOV3c.2 cell line was used because this subclone of SKOV3 was tumorigenic subcutaneously and expressed a relatively higher level of SYK (Figure 2D). Athymic mice bearing the SKOV3c.2 subcutaneous tumors were treated with paclitaxel (8 mg/kg), R406 (6.5 mg/kg), or the combination. Drugs were administered over several 3 days on/3 days off cycles initiated when the tumors first became palpable (Figure S4A). We intended to use a low dose of paclitaxel and R406 to determine the combinational anti-tumor effect and minimize adverse effects. At the given doses, there was no significant difference in tumor weight between the control group and the groups treated with either single R406 or paclitaxel after four cycles of treatment (Figures 4A–4C). However, a significant reduction in tumor weight was recorded in the group co-treated with R406 and paclitaxel compared to the control group ($p < 0.0004$). The percentage of tumor cells that incorporated bromodeoxyuridine (BrdU) was significantly lower in tumors receiving the combined R406 and paclitaxel than in other groups ($p = 0.01$) (Figure 4B). R406-treated tumors in mice showed a reduction of the p-SYK (Y525/526)/SYK ratio (Figure S4B). No significant differences were detected between groups treated with R406 alone and paclitaxel alone. Body weight, physical activity, and splenic weight of mice in these groups were similar (Figures S4C and S4D).

Next, we determined if the paclitaxel and R406 combination was effective in suppressing intraperitoneal tumor growth in an in vivo paclitaxel-resistant ovarian cancer model. We established intraperitoneal SKOV3^{Luc} tumors in mice that recurred after continuous paclitaxel treatment for 7 weeks (Figure 4D). Compared to tumors grown in mice treated with vehicle, tumors that recurred in mice treated with paclitaxel showed higher levels of p-SYK (Y525/526) and SYK (Figure S4E). In primary cultures, cells from recurrent paclitaxel-treated tumors were more resistant to paclitaxel than cells from vehicle-treated tumors (Figure 4D). The cells from the paclitaxel-resistant tumor (paclitaxel-1) were then re-injected intraperitoneally in a new cohort of mice followed by treatment with either vehicle, R406, paclitaxel or the combination. The new xenografts responded to paclitaxel initially, but regrew after week 3. Paclitaxel and R406 combination significantly reduced tumor progression in this model as compared to paclitaxel alone at week 4 and 5. R406 alone at the applied dose did not show any anti-tumor effect as compared to vehicle control (Figures 4E and 4F). Similar to a previous report (Braselmann et al., 2006), we did not detect gross or microscopic abnormalities in organs from these R406-treated mice. The above results indicate that the combination of paclitaxel and R406 effectively inhibited tumor growth at doses that were highly tolerable in mice.

Identification of Substrates Phosphorylated by SYK in Paclitaxel-Resistant Tumor Cells

To elucidate the molecular mechanisms by which SYK inhibition enhanced cytotoxic effects of paclitaxel, we performed stable isotope labeling by amino acids in cell culture (SILAC) (Ong et al., 2002) and compared the phosphoproteome between SKOV3TR cells treated with R406 and vehicle control. Based on two independent experiments, we identified 896 unique, differentially expressed phosphopeptides corresponding to 516 proteins (Table S2), more than 90% of which belonged to phosphotyrosine-containing peptides. Because we were interested in those proteins that were potentially phosphorylated by SYK, we focused on the phosphorylation sites that were downregulated (average H/L ratio <0.7) by R406 in duplicate experiments. As a result, there were 327 downregulated phosphopeptides belonging to 228 proteins. Among them, 141 peptides contained at least one acidic residue surrounding the phosphorylated Tyr, and were, therefore, considered potential substrates for SYK (Xue et al., 2012, 2013). Several SYK substrates identified in this study, including SYK itself and PLCG1, LCK, STAT3, and α-tubulin, have been previously reported to be SYK substrates in hematopoietic cells (Couture et al., 1996; Law et al., 1996; Peters et al., 1996; Uckun et al., 2010b). This finding indicated the robustness of our approach in identifying SYK substrates in ovarian cancer cells.

Pathway analysis indicated that the identified SYK substrates participate in cell motility and organization of cytoskeleton in addition to proliferation/growth, cell death, and survival among other processes (Figures 5A–5C). Specifically, we identified 19 phosphosites (Table 1) in the following proteins: dynactin 2 (DCTN2), microtubule-associated protein 1B (MAP1B), microtubule-associated protein 4 (MAP4), tubulin binding co-factor B (TBCB), α-tubulin, and β-tubulin, all of which are proteins essential for microtubule dynamics. Table S3 lists phosphopeptides we identified that were also reported in B lymphocytes and breast cancer cells in a recent study that used an independent method (Xue et al., 2012).

We selected representative SYK substrates including α-tubulin, β-tubulin, MAP4, and MAP1B for further validation because these proteins are constituents of the microtubules, and their posttranslational modification such as phosphorylation may have a direct impact on microtubule stability. Consistent with a previous report (Faruki et al., 2000), we were able to demonstrate phosphorylation of tubulin by SYK. Importantly, our data from an in vitro kinase assay using active recombinant SYK and purified bovine microtubule-associated protein (MAPs) demonstrated that MAP1B and MAP4 were substrates of SYK (Figure 5D). Furthermore, co-immunoprecipitation assays demonstrated that SYK inhibitors (R406 and GS-9973) reduced the levels of Tyr-phosphorylated α- and β-tubulin, although the

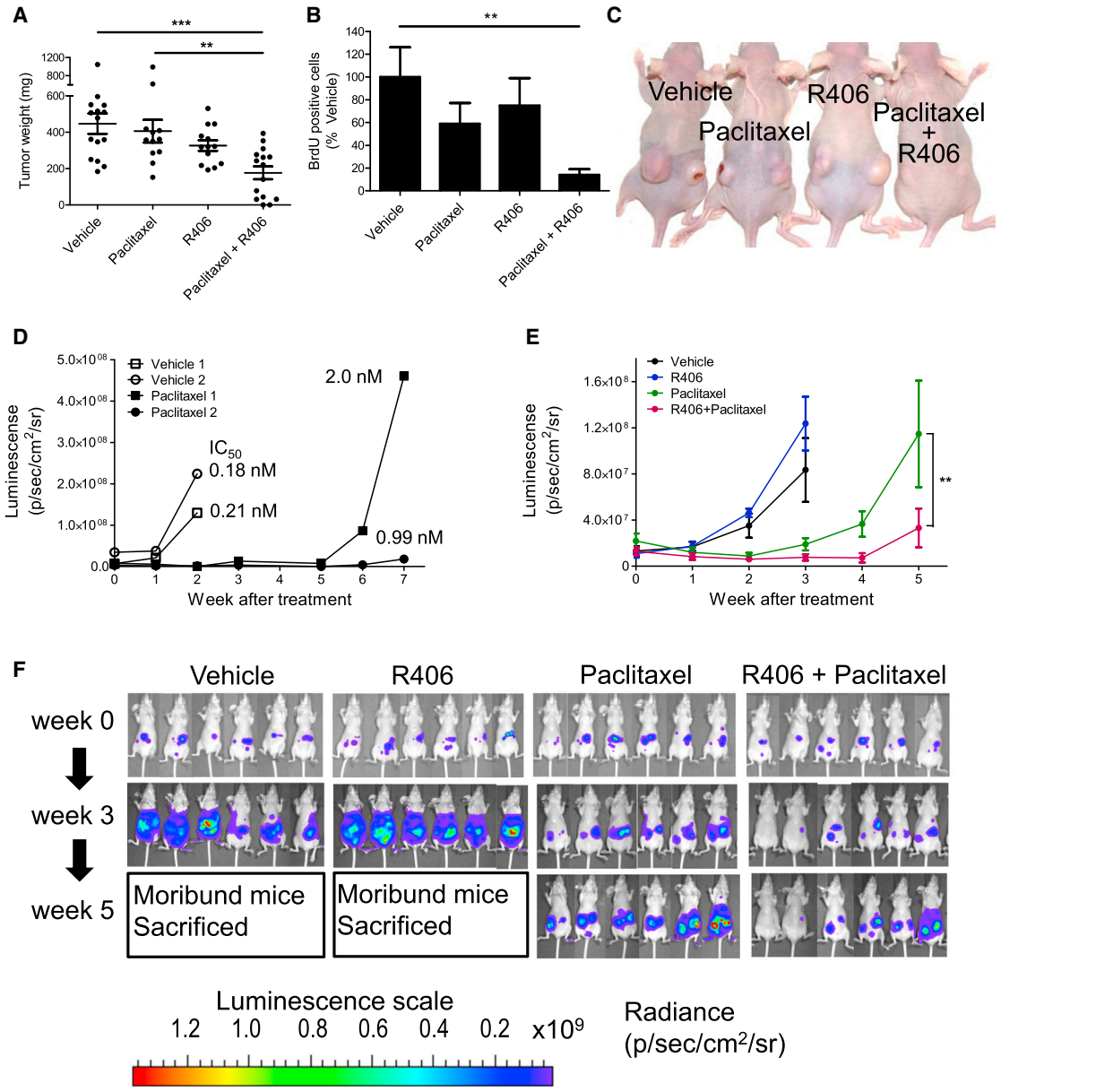

Figure 4. Combination of Paclitaxel and R406 Decreases Tumor Growth in Mice

(A–C) Tumor weights (A), BrdU incorporation into tumors (B), and representative tumor-bearing mice (C) of the SKOV3c.2 subcutaneous tumor model treated as indicated. Tumor weights are plotted and analyzed by one-way ANOVA followed by Tukey's post hoc test.

(D) The growth of intraperitoneal SKOV3^{Luc} tumors in vehicle-treated (vehicles 1 and 2) and in paclitaxel-treated (paclitaxel 1 and 2) mice. Paclitaxel IC_{50} values of the tumors from the four mice were determined in individual primary cultures.

(E) Mice injected intraperitoneally with cells isolated from the paclitaxel-1 tumor were treated as indicated and the luminescence signals were analyzed by two-way ANOVA with Bonferroni posttests.

(F) The luminescence of the intraperitoneal SKOV3^{Luc} tumor xenografts from different treatment groups at the indicated week. $^{**}p < 0.01$; $^{***}p < 0.001$. Results are shown as ± SEM. See also Figure S4.

effect of P505-15 was modest. The induction of MAP4 and MAP1B Tyr phosphorylation by the Tyr phosphatase inhibitor pervanadate, which is known to activate SYK signaling (Faruki et al., 2000), was suppressed by SYK inhibitors (Figure S5A). SYK knockdown by siRNA demonstrated a similar result (Figure S5B). Collectively, these data show that tubulin and MAPs are direct SYK substrates.

Next, we compared the expression of total and Tyr-phosphorylated α- and β-tubulin, MAP4, and MAP1B between paclitaxel-sensitive (SKOV3 and MPSC1) and paclitaxel-resistant cells (SKOV3TR and MPSC1TR) cells. Consistent with an elevated SYK level in paclitaxel-resistant cells, Tyr-phosphorylated α-tubulin (Figure 5E), but not Tyr-phosphorylated β-tubulin, was upregulated in these resistant cells (Figure S5C). Similarly,

total MAP1B and its Tyr-phosphorylated form were also upregulated in the paclitaxel-resistant cells (Figure 5E). In a panel of ovarian cancer cell lines, higher expression levels of ptyr-MAP1B/MAP1B were associated with less sensitivity to paclitaxel (Figures 5F and S5D), further suggesting the involvement of MAP1B tyrosine phosphorylation in paclitaxel resistance. Using immunohistochemistry with the antibody against phospho-α-tubulin (Y272) in 161 HGSC samples, we observed a positive correlation in staining intensity between total SYK and phospho-tubulin, and between phospho-SYK and phospho-α−tubulin (Figure 5G). Two representative cases with high and low staining intensity of SYK, phospho-SYK, and phospho-α-tubulin are shown in Figure 5H.

Expression of Active SYK Confers Paclitaxel Resistance and Increases MAP1B and MAP4 Tyrosine Phosphorylation

To demonstrate whether activating the SYK pathway is sufficient to confer paclitaxel resistance, we generated tetracycline-inducible SKOV3 cells to ectopically express wild-type or active SYK mutant (SYK-130E), which has been shown to have a high basal kinase activity (Keshvara et al., 1997). Paclitaxel IC_{50} significantly increased in ovarian cancer cells after induction of SYK-130E, and to a lesser extent of SYK (Figures 6A and 6B), indicating that SYK activation is sufficient to render paclitaxel resistance. Moreover, cells expressing constitutively active SYK-130E demonstrated increased Tyr-phosphorylated MAP1B and MAP4, but not tubulin (Figure 6C). Using an in vitro microtubule binding assay, we observed that SYK phosphorylated MAP1B and MAP4 could still bind microtubule (Figure S6, comparing SYK 0.4 μg sample plus/minus ATP), but the presence of R406 further increased their binding.

SYK Inhibition Stabilizes Microtubules in Paclitaxel-Resistant Tumor Cells Co-treated with Paclitaxel

Two different approaches were used to determine whether inhibiting SYK activity would stabilize microtubules. First, we assessed two markers of microtubule stability, acetylated α-tubulin (L'Hernault and Rosenbaum, 1985; Piperno and Fuller, 1985) and detyrosinated (Glu) α-tubulin (Gundersen et al., 1984; Thompson, 1977). Western blot analysis demonstrated that paclitaxel markedly increased both acetylated and detyrosinated tubulin levels in paclitaxel-sensitive SKOV3 and MPSC1 cells, but the effect was only modest in paclitaxel-resistant SKOV3TR and MPSC1TR cells (Figure 7A), indicating that the paclitaxel-resistant cells had developed a mechanism(s), presumably by increasing phosphorylation of tubulin and MAPs (Figure 5E), to counteract paclitaxel-induced microtubule stability. Neither acetylated nor detyrosinated tubulin levels were altered by R406 alone at the applied concentration (2.5 μM) in either paclitaxel-resistant cell line, although R406 at a higher concentration increased the levels of acetylated α-tubulin in paclitaxel-sensitive and -resistant SKOV3 cells (Figure S7A). Compared to vehicle control, R406 alone, and paclitaxel alone, R406 and paclitaxel combination significantly increases the level of acetyl-α-tubulin in SKOV3TR and MPSCTR cells. This finding was not observed in naive cells because they are highly sensitive to paclitaxel in stabilizing microtubules at the given paclitaxel concentration (Figure 7A). Combination with other SYK inhibitors showed similar results (Figure S7B). The above findings were confirmed by immunofluorescence (Figure S7C). Ovarian cancer cell lines, KK, KOC7C, and OVTOKO, all of which were more resistant to paclitaxel than the naive SKOV3 and MPSC1 cells showed similar enhancement of acetylated α-tubulin in the combination treatment (Figure 7A). To further extrapolate the finding to an in vivo setting, we compared levels of acetyl-α-tubulin in SKOV3c.2 tumor xenografts in mice treated with paclitaxel, R406, or their combination. We observed a significant increase in the acetylated-α-tubulin level in tumor xenografts treated with combined R406 and paclitaxel (Figure 7B). The results of these experiments suggested that inhibition of SYK in the presence of paclitaxel augmented microtubule stabilization and cytotoxicity in paclitaxel-resistant tumor cells that were otherwise insensitive to paclitaxel.

In the second approach, we applied live-cell microscopy to record microtubule dynamics in SKOV3 and SKOV3TR cells stably transfected with GFP-α-tubulin. We used the fluorescence recovery after photobleaching (FRAP) technique to measure the speed of microtubule turnover in these cells. We observed that cells treated with R406 alone (2.5 μM) did not show any detectable changes in fluorescence recovery in SKOV3 cells. As expected, SKOV3 cells responded to paclitaxel treatment with a reduced mobile fraction and an increased half-life after photobleaching (Figure 7C). In contrast, SKOV3TR cells were less responsive to paclitaxel, but adding R406 (2.5 μM) to paclitaxel (30 nM) significantly reduced fluorescence recovery, including a decreased mobile fraction and an increased half-life (Figure 7D). In SKOV3TR cells, R406 alone only slightly increased the half-life of fluorescence recovery and did not have a significant effect on mobile fractions. Thus, FRAP analysis confirmed that SYK inactivation promoted paclitaxel-induced stabilization of microtubules in paclitaxel-resistant cancer cells.

DISCUSSION

This study provides biological basis and pre-clinical evidence that targeting SYK sensitizes tumor cells to paclitaxel, especially for those that have developed paclitaxel resistance. It is likely that the paclitaxel-resistant cells with higher SYK levels and activity have developed a molecular mechanism that counteracts paclitaxel-mediated microtubule stabilization, thus reducing paclitaxel-induced cytotoxicity. Our finding validates a previous hypothesis that modulating microtubule stability can enhance the cytotoxic response of ovarian cancer cells to paclitaxel (Ahmed et al., 2011). Indeed, by analyzing the SYK substrates in paclitaxel-resistant ovarian cancer cells, we identified tubulin and MAPs as substrates of SYK, raising the possibility that SYK inactivation affects microtubule dynamics. The role of SYK in cancer therapeutics has also been reported by others. SYK activity has been demonstrated to play an important role in imatinib or nilotinib resistance in CML (Gioia et al., 2011) and the pentapeptide mimic targeting the substrate binding site of SYK has an anti-tumor effect on chemotherapy-resistant relapsed B-precursor leukemia cells (Uckun et al., 2010a).

How SYK tyrosine phosphorylation affects the functions of tubulin and MAPs is not clear. Faruki et al. reported that tubulin, upon SYK-mediated phosphorylation, was able to assemble into microtubules (Faruki et al., 2000), but the effects on microtubule

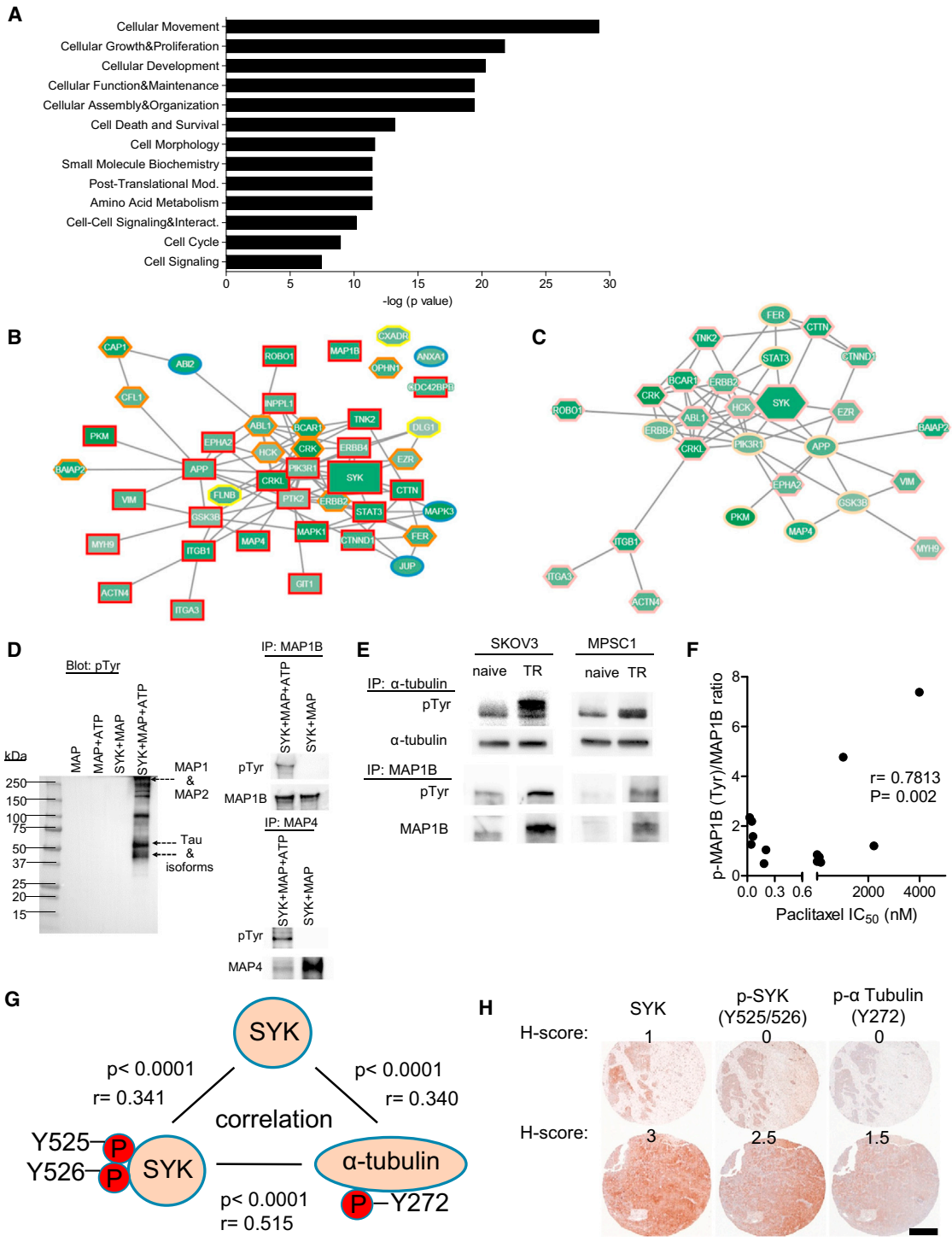

Figure 5. Phosphoproteomic Analyses Identify SYK Substrates Including Those Involved in Organization of Cytoskeleton

(A) Ingenuity pathway analysis showing that cellular functions participate via phosphoproteins downregulated by R406.

(B) Interactome network shows that phosphoproteins downregulated by R406 are largely involved in regulating microtubule dynamics and organizing actin cytoskeleton. Rectangle nodes with red borders represent microtubules dynamics; the octagon nodes with yellow border represent organization of actin cytoskeleton; and the hexagon nodes with orange borders represent organization of microtubules dynamics and the organization of actin cytoskeleton. The lines between nodes are known protein-protein interactions in the PPI database.

(C) Interactome network of phosphoproteins involved in microtubule stabilization. Ellipse nodes represent proteins that stabilize microtubules. The lines between nodes are known protein-protein interactions in the PPI database.

(legend continued on next page)

dynamics remain to be determined. This is further complicated by SYK-mediated phosphorylation on many microtubule interacting proteins such as MAP1B and MAP4 that also play critical roles in microtubule dynamics (Krisenko et al., 2014). MAP1B and MAP4 bind to microtubules and facilitate their polymerization and stabilization. Because serine phosphorylation of MAPs has been shown to decrease interactions of MAPs and microtubules, promoting microtubule dynamics (Chang et al., 2001; Goold et al., 1999; Trivedi et al., 2005), it is likely that tyrosine phosphorylation by SYK has a similar effect because SYK phosphorylates MAP4 at tyrosine Y1001, which resides in the conserved microtubule binding domain of MAP4.

The observation that R406 alone is sufficient to reduce cellular proliferation at doses that do not significantly affect microtubule stability suggests that the anti-proliferative activity of R406 can also be attributed to inactivation of SYK-regulated tumor-promoting pathways. By analyzing the SILAC data, we also identified several SYK substrates that belong to canonical tumor-promoting pathways. These include STAT3, which has been reported as a substrate for SYK in hematopoietic cells (Uckun et al., 2010b). R406 markedly reduces phosphorylation of STAT3 tyrosine residues Y704 and Y705, the latter of which is associated with STAT3 activity and its anti-apoptotic effect (Chen et al., 2008). In addition, we identified a group of SYK substrates including PIK3R1/2 and adaptor proteins, GAB1/2 and SHC, that are involved in the growth factor/PI3K signaling. These proteins generally couple signaling among activated growth factor receptors upon ligand binding such as VEGF, EGF, IGF1, and HGF (Holgado-Madruga and Wong, 2003) with PI3K signaling pathway, which has been known to participate in chemoresistance (Koti et al., 2013). Thus, our data suggest that the anti-tumor effects of inactivating SYK come from two broad mechanisms—stabilizing microtubules and suppressing growth-promoting signaling pathways. For the latter, we demonstrated that R406 suppressed phosphorylation of other SYK substrates including pSTAT3 and pAKT of which phosphorylation was reported to protect tumor cells from chemotherapy-induced cytotoxicity. However, unlike the synergistic effect on microtubule stability, adding paclitaxel did not further reduce their phosphorylation levels (data not shown). Thus, we focus on the biological effects of targeting SYK signaling on microtubule dynamics.

Microtubules have been well established as a major target for cancer treatment. The anti-mitotic microtubule-targeting drugs include (1) vinca alkaloids (vinblastine, vincristine, vindesine, and vinorelbine) that bind to α– and β-tubulin heterodimers, preventing their incorporation into microtubules and microtubule polymerization; and (2) microtubule-stabilizing agents such as paclitaxel and docetaxel (collectively known as taxanes) that directly interact with and stabilize microtubules (Liu et al., 2014). Thus, SYK inhibitors represent another group of drugs that affect microtubules through regulating phosphorylation of tubulin and MAPs. The different mechanisms used by SYK inhibitors and paclitaxel may explain their synergistic effect in cancer cells, especially in those that developed paclitaxel resistance. Our results may have important clinical ramifications because taxanes are frequently used in treating several major types of cancer such as breast and lung carcinoma in addition to ovarian carcinoma. Because development of taxane resistance is common, introduction of regimens to overcome paclitaxel resistance is an unmet need.

The main SYK inhibitor used in this study is R406, the active form of fostamatinib (also known as R788), which is orally administrable and highly tolerable when used in late-phase clinical trials of rheumatoid arthritis, auto-immune diseases, and hematologic malignancies (Friedberg et al., 2010; Podolanczuk et al., 2009; Weinblatt et al., 2010). Several clinical trials of fostamatinib have reported its pharmacokinetics and safety profile at a range of doses up to 250 mg twice daily (Friedberg et al., 2010; Weinblatt et al., 2008). The plasma concentration reported from these studies ranges between 300 and 1,800 ng/ml (molar concentration 0.5–2.9 μM), which is relevant to the R406 concentrations used in our experiments. Therefore, the availability of fostamatinib and the minimal overlap between observed clinical toxicities of fostamatinib and paclitaxel would facilitate the translation of the current pre-clinical study (Weinblatt et al., 2010). For example, results of our study warrant determining the benefit of adding fostamatinib to the weekly paclitaxel regimen used in treating recurrent ovarian cancer.

Finally, the current study focuses on demonstrating the direct function of SYK on microtubule constituents and concludes that the major mechanism for SYK inhibitors to sensitize paclitaxel effects is through altering the SYK-MAP-tubulin axis. Because SYK may have multiple roles in promoting tumor progression, it should not be construed that other SYK-regulated microtubule-independent pathways are not involved in paclitaxel resistance. In fact, this study also validated that both STAT3 and AKT were the substrates of SYK and their inhibition can enhance cytotoxicity of chemotherapeutic agents, although the underlying mechanisms have yet to be further elucidated (Lin et al., 2015; Abubaker et al., 2014).

EXPERIMENTAL PROCEDURES

Detailed materials and methods are provided in the Supplemental Experimental Procedures.

Immunohistochemistry

Formalin-fixed and paraffin-embedded ovarian cancer tissues were obtained from the Department of Pathology at the Johns Hopkins Hospital, Baltimore,

(D) In vitro kinase assay using recombinant active SYK and purified bovine microtubule-associated protein (MAP). Immunoprecipitation was used to enrich MAP1B and MAP4.

(E) Tyr-phosphorylated (pTyr) and total α-tubulin and MAP1B in naive and paclitaxel-resistant (TR) SKOV3 and MPSC1 cells. For the IP: MAP1B panels, the naive and paclitaxel-resistant cells for each cell line were blotted on the same membrane but not on the adjacent lane. The images were cropped to allow side-by-side comparison of the naive and paclitaxel-resistant conditions.

(F) Pearson correlation analysis between Tyr-phosphorylated MAP1B/MAP1B ratio and sensitivity to paclitaxel in a group of ovarian cancer cell lines.

(G) Correlation between the levels of total and phospho-SYK and phospho-tubulin (Y272) using immunohistochemistry in 161 ovarian carcinomas.

(H) Representative images of SYK, phospho-SYK (Y525/526), and phospho-α tubulin (Y272) immunostaining. Scale bar represents approximately 400 μm. See also Figure S5 and Tables S2 and S3.

Table 1. Candidate of SYK Substrates Related to Microtubules

Gene Symbol	Full Name	Accession	Phosphopeptide	Protein Phosphorylation Site	Exp. 1 H/L Ratio	Exp. 2 H/L Ratio
DCTN2	dynactin 2 (p50)	NP_006391	TGYESGEyEMLGEGLGVK	Y91	0.50	0.72
MAP1B	microtubule-associated protein 1B	NP_005900	AAEAGGAEEQyGFLTTPTK	Y1062	0.37	0.59
			SPPLIGSESAyESFLSADDKASGR	Y1410	0.47	0.89
			ESSPLySPTFSDSTSAVK	Y1796	0.34	0.64
			ESsPLySPTFSDSTSAVK	Y1796, S1793	0.32	0.57
			TSDVGGYYyEK	Y1906	0.47	0.67
			SPSDSGySYETIGK	Y1921	0.41	0.70
			SPSDSGYSyETIGK	Y1923	0.37	0.70
			TPEDGDySYEIIEK	Y1938	0.47	0.41
			TPEDGDYSyEIIEK	Y1940	0.44	0.65
			TPDTSTyCYETAEK	Y2040	0.40	0.65
			TPDTSTYCyETAEK	Y2042	0.40	0.65
			TATCHSSSSPPIDAASAEPyGFR	Y1830	0.27	0.64
			TPEEGGySYDISEK	Y1955	0.40	0.50
			TTKTPEDGDySYEIIEK	Y1938	0.49	0.64
			VLSPLRsPPLIGSESAyESFLSADDK	Y1410, S1400	0.23	0.44
			YESSLYSQEySKPADVTPLNGFSEGSK	Y1174	0.36	0.48
MAP4	microtubule-associated protein 4	NP_002366	KVSySHIQSK	Y1001	0.34	0.74
TBCB	tubulin folding co-factor B	NP_001272	LGEyEDVSR	Y98	0.52	0.94
TUBA4A	tubulin α-4A	NP_005991	IHFPLATyAPVISAEK	Y272	0.30	0.48
TUBA3E	tubulin α-3E	NP_997195				
TUBA3D	tubulin α-3D	NP_525125				
TUBA3C	tubulin α-3C	NP_005992				
TUBA1C	tubulin α-1C	NP_116093				
TUBA1B	tubulin α-1B	NP_006073				
TUBA1A	tubulin α-1A	NP_006000				
TUBA8	tubulin α-8	NP_061816	QLFHPEQLITGKEDAANNyAR	Y103	0.38	0.69
TUBA4A	tubulin α-4A	NP_005991				
TUBA3D	tubulin α-3D	NP_525125				
TUBA3C	tubulin α-3C	NP_005992				
TUBA1C	tubulin α-1C	NP_116093				
TUBA1B	tubulin α-1B	NP_006073				
TUBA1A	tubulin α-1A	NP_006000				
TUBA8	tubulin α-8	NP_061816	VGINyQPPTVVPGGDLAK	Y357	0.34	0.43
TUBA4A	tubulin α-4A	NP_005991				
TUBA3E	tubulin α-3E	NP_997195				
TUBA3D	tubulin α-3D	NP_525125				
TUBA3C	tubulin α-3C	NP_005992				
TUBA1C	tubulin α-1C	NP_116093				
TUBA1B	tubulin α-1B	NP_006073				
TUBA1A	tubulin α-1A	NP_006000				
TUBB	tubulin β	NP_821133	ISVYyNEATGGK	Y51	0.45	0.57
TUBB	tubulin β	NP_821133	NSsYFVEWIPNNVK	Y340	0.49	0.43
TUBB6	tubulin β-6	NP_115914				
TUBB4A	tubulin β-4A	NP_006078				
TUBB3	tubulin β-3	NP_006077				
TUBB4B	tubulin β-4B	NP_006079				
TUBB2B	tubulin β-2B	NP_821080				

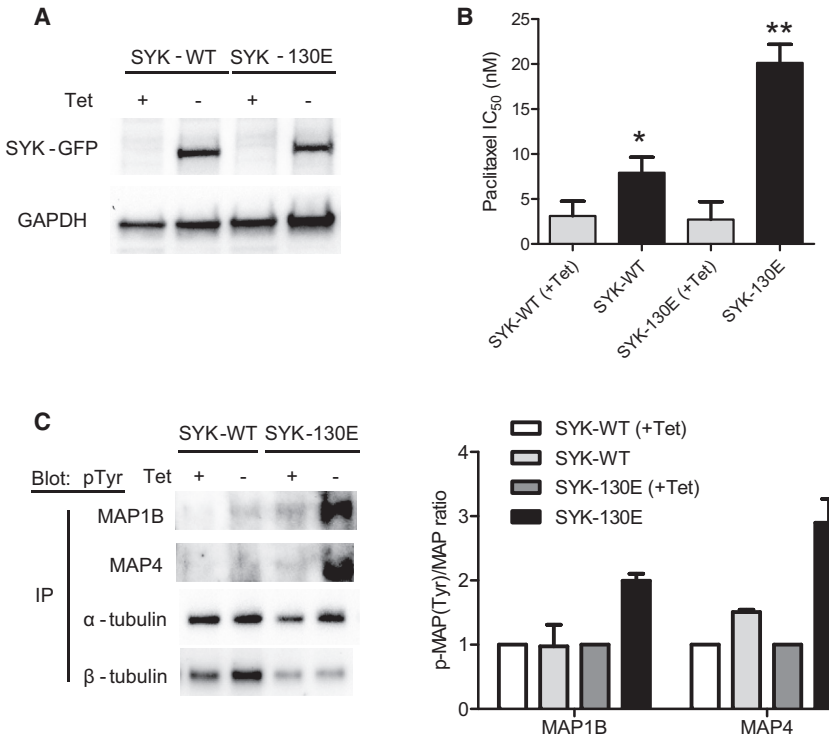

Figure 6. Effects of Ectopic SYK Expression on Paclitaxel Sensitivity and Tyrosine Phosphorylation of MAP1B and MAP4 in SKOV3

(A) Western blot analysis shows expression of ectopic SYK-WT and SYK-130E with and without induction.

(B) Paclitaxel IC_{50} in cells expressing ectopic SYK-WT and SYK-130E as compared to non-induced cells (+Tet). *$p < 0.05$; **$p < 0.01$ as determined by one-way ANOVA with Tukey's post hoc test.

(C) MAP1B and MAP4 tyrosine phosphorylation in SYK-130E-expressing cells. Results are shown as mean ± SEM. See also Figure S6.

Maryland. All studies were Johns Hopkins University School of Medicine Institutional Review Board exempt because no protected health information was used. To compare the expression levels of SYK in paired recurrent post-chemotherapy ovarian HGSC and their primary untreated tumors, we performed immunohistochemistry. The primary tumors from HGSC patients were optimally debulked to a residual tumor volume less than 1 cm, and all patients received standard carboplatin and paclitaxel therapy for three to six cycles. Paraffin tissues were arranged in tissue microarrays to facilitate immunohistochemistry and to ensure that tissues were stained under the same conditions. The 214 effusions were obtained from the Norwegian Radium Hospital (177 peritoneal, 37 pleural) were from 211 patients (two patients had two effusions) diagnosed with serous carcinoma in the years 1998–2005. One hundred twenty-three effusions were collected at diagnosis prior to chemotherapy, whereas 88 effusions were post-chemotherapy specimens, collected at disease recurrence. Data regarding previous chemotherapy were unavailable for three patients. The FIGO stages were one patient with stage I, four with stage II, 127 with stage III, and 82 with stage IV disease. Residual tumor volume was ≤1 cm in 86 cases, >1 cm in 95 cases, and unknown in 33 cases. The majority of patients (n = 193) received platinum-based chemotherapy at diagnosis. Chemotherapy response was classified as complete response, 117 patients; partial response, 31 patients; stable disease, 12 patients; and progression, 28 patients. The disease response after chemotherapy for the remaining cases (n = 23) could not be evaluated because of adverse effects, normal CA-125 after primary surgery or missing CA-125 information and no grossly residual tumor. The study was approved by the Regional Committee for Medical Research Ethics in Norway. Comparative analysis was performed for patients with complete response versus partial response/stable disease/progression. The statistical program used was SPSS version 18. The test for association with chemotherapy response was Mann-Whitney.

The mouse monoclonal anti-SYK antibody [4D10.1] (Abcam ab3113), anti-phospho-SYK (Tyr525/526) antibody (CST #2711), and anti-α-tubulin (phospho Y272) antibody [EP1334(2)Y] (Abcam ab76290) were used, and their specificity was confirmed by western blotting. The specificity of anti-phospho-SYK (Y525/526) antibody in immunohistochemistry was previously validated using anti-BCR stimulated B-lymphoma cells and tissues (Cheng et al., 2011). Citrate-based Target Retrieval Solution (DAKO) was used for antigen retrieval (95°C–100°C for 20 min). The sections were then incubated with the primary antibody at 4°C overnight and the appropriate secondary antibody at room temperature for 30 min. Colorimetric development was detected by the EnVision+System (DAKO). Sections were counterstained with hematoxylin, and immunoreactivity was scored using the H score system by two investigators based on the percentage of positively stained cells and the intensity of staining, which ranged from 0 to 3+. A composite score was determined by multiplying the intensity and extent scores.

Xenograft Mouse Tumor Models

Two models were used in this study. In the subcutaneous tumor model, a tumorigenic line of SKOV3 cells, SKOV3c.2 cells, were mixed with an equal volume of Matrigel (BD Biosciences) and injected subcutaneously (5×10^6 cells/injection) into female *nu/nu* mice. Tumor growth was monitored by measurements of tumor diameters, and the tumor volume was calculated. Treatment with drugs started as soon as the tumor became palpable. At the end of treatment, all tumors were excised, weighed, and confirmed by histology. For BrdU incorporation, mice were intraperitoneally injected with 150 mg/kg and killed 2 hr post-injection. Tumor cells that had incorporated BrdU were detected in paraffin-embedded sections with an anti-BrdU antibody. The number of total tumor cells and positively stained tumor cells were counted.

In the intraperitoneal tumor model, SKOV3 luciferase expressing cells (5×10^6) were injected intraperitoneally into female *nu/nu* nude mice. Paclitaxel treatment was initiated when luminescence signal reached $>2 \times 10^6$ photons/s. Mice were treated with vehicle (control) or paclitaxel intraperitoneally three times per week for up to 7 weeks. Tumor burden was measured weekly in mice injected with d-luciferin using the IVIS Spectrum In Vivo Imager. IC_{50} of paclitaxel was determined in primary cultures established from individual tumors. Paclitaxel-resistant cells were expanded and re-injected intraperitoneally into a new cohort of mice to examine the anti-tumor activity of single-agent R406, paclitaxel, or the combination. When tumor luminescence signals exceeded 2×10^6 photons/s, mice received intraperitoneal administration of vehicle control, R406 (10 mg/kg), paclitaxel (10 mg/kg), or the combination three times per week. All of the animal procedures were approved by the Johns Hopkins University Animal Care Committee.

Fluorescence Recovery after Photobleaching

SKOV3 and SKOV3TR cells were transfected with a plasmid expressing GFP-α-tubulin, and multiple positive clones were pooled for further expansion. Photobleaching procedures were performed using a confocal laser-scanning microscope. The dynamics parameters recorded from FRAP included the fraction of microtubules that recovered within 2 min after photobleaching (mobility fraction), and the time it took for half of the mobile fraction of microtubules to recover ($t_{1/2}$). Regions of interest were bleached for 10 s followed by 2 min of observation, with image acquisition every 2 s. At least 12–15 observations were recorded per sample, and the recovered fluorescence intensities were normalized against background and unbleached regions within the cell of interest (Daniels et al., 2009).

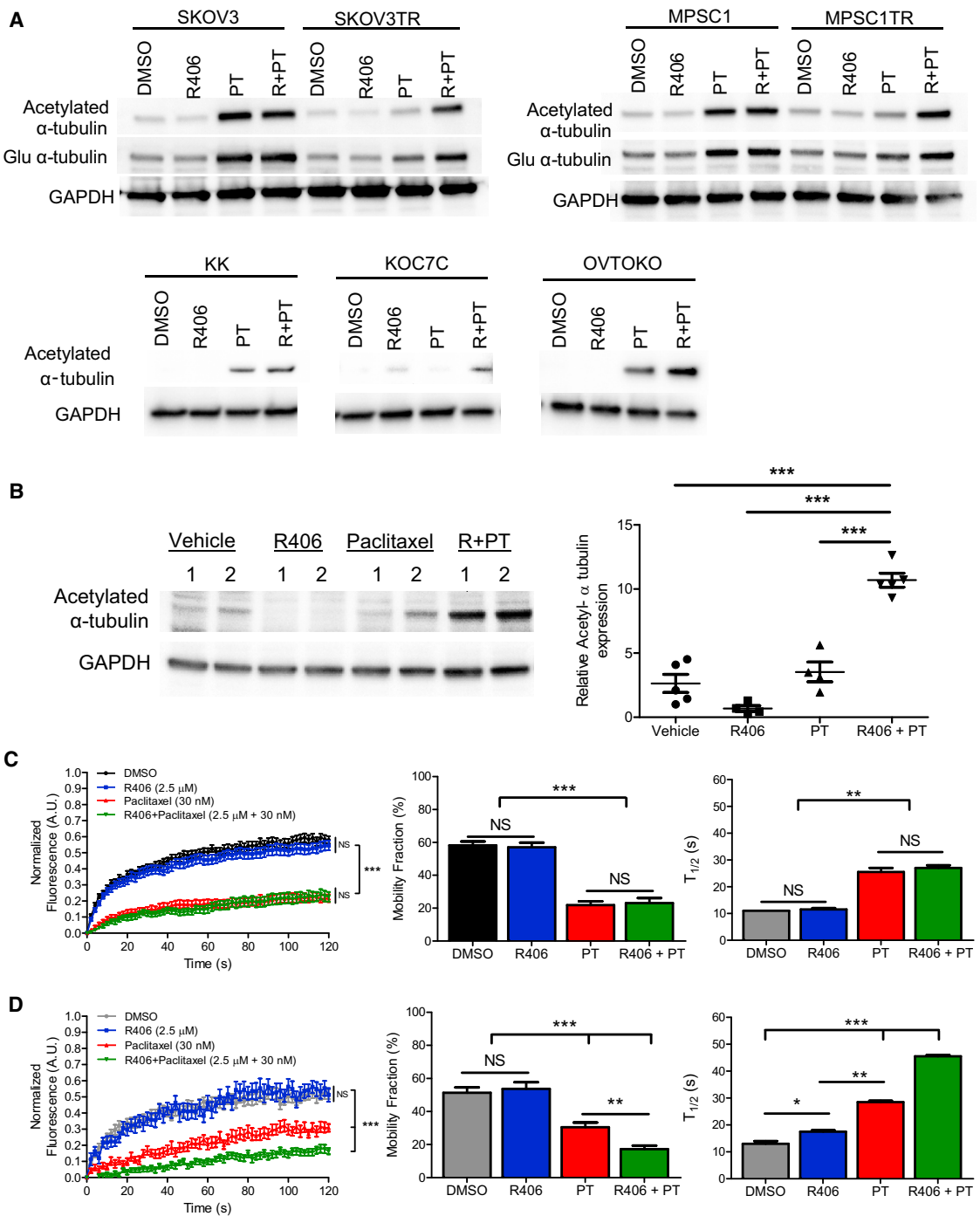

Figure 7. Combination of SYK Inhibitor and Paclitaxel Results in Microtubule Stabilization in Paclitaxel-Resistant Ovarian Cancer Cells

(A) Immunoblottings of acetyl or detyrosinated tubulin after treatment with DMSO, R406 (2.5 μM), paclitaxel (30 nM), or a combination of R406 (2.5 μM) and paclitaxel (30 nM) in indicated cell lines.

(B) Immunoblotting analysis of acetyl-α-tubulin in tumor xenografts (two representative tumors from each group) comparing combination of R406 and paclitaxel to vehicle or single agents. Statistical significance is determined by one-way ANOVA with Tukey's post hoc test. ***$p < 0.001$.

(C and D) FRAP assay analysis of mobility fraction between the group treated with paclitaxel and the group co-treated with R406 and paclitaxel in SKOV3 cells (C) and SKOV3TR cells (D). Mobility fraction and $T_{1/2}$ were analyzed by one-way ANOVA with Tukey's post hoc test. *$p < 0.05$; **$p < 0.01$; ***$p < 0.001$. Results are shown as ± SEM. See also Figure S7.

SUPPLEMENTAL INFORMATION

Supplemental Information includes Supplemental Experimental Procedures, seven figures, and three tables and can be found with this article online at http://dx.doi.org/10.1016/j.ccell.2015.05.009.

ACKNOWLEDGMENTS

This work was supported by RO1CA103937 (to I.-M.S.), W81XWH-11-2-0230/OC100517 (to I.-M.S.), RO1CA148826 (to T.-L.W.), R21CA187512 (to T.-L.W.), R01CA174388 (to D.W.), U54CA143868 (to D.W.), NCI's Clinical Proteomic Tumor Analysis Consortium (CPTAC) initiative (U24CA160036 to A.P. and I.-M.S.), Conquer Cancer Foundation 2011 Young Investigator Award (to S.G.), HERA OSB Grant from the HERA Women's Cancer Foundation (to Y.Y.), and Ovarian Cancer Research Fund 292512 (to Y.Y.).

Received: November 6, 2014
Revised: March 11, 2015
Accepted: May 12, 2015
Published: June 18, 2015

REFERENCES

Abubaker, K., Luwor, R.B., Escalona, R., McNally, O., Quinn, M.A., Thompson, E.W., Findlay, J.K., and Ahmed, N. (2014). Targeted disruption of the JAK2/STAT3 pathway in combination with systemic administration of paclitaxel inhibits the priming of ovarian cancer stem cells leading to a reduced tumor burden. Front Oncol *4*, 75.

Ahmed, A.A., Wang, X., Lu, Z., Goldsmith, J., Le, X.F., Grandjean, G., Bartholomeusz, G., Broom, B., and Bast, R.C., Jr. (2011). Modulating microtubule stability enhances the cytotoxic response of cancer cells to Paclitaxel. Cancer Res. *71*, 5806–5817.

Braselmann, S., Taylor, V., Zhao, H., Wang, S., Sylvain, C., Baluom, M., Qu, K., Herlaar, E., Lau, A., Young, C., et al. (2006). R406, an orally available spleen tyrosine kinase inhibitor blocks fc receptor signaling and reduces immune complex-mediated inflammation. J. Pharmacol. Exp. Ther. *319*, 998–1008.

Buchner, M., Fuchs, S., Prinz, G., Pfeifer, D., Bartholomé, K., Burger, M., Chevalier, N., Vallat, L., Timmer, J., Gribben, J.G., et al. (2009). Spleen tyrosine kinase is overexpressed and represents a potential therapeutic target in chronic lymphocytic leukemia. Cancer Res. *69*, 5424–5432.

Chang, W., Gruber, D., Chari, S., Kitazawa, H., Hamazumi, Y., Hisanaga, S., and Bulinski, J.C. (2001). Phosphorylation of MAP4 affects microtubule properties and cell cycle progression. J. Cell Sci. *114*, 2879–2887.

Chen, C.L., Cen, L., Kohout, J., Hutzen, B., Chan, C., Hsieh, F.C., Loy, A., Huang, V., Cheng, G., and Lin, J. (2008). Signal transducer and activator of transcription 3 activation is associated with bladder cancer cell growth and survival. Mol. Cancer *7*, 78.

Cheng, S., Coffey, G., Zhang, X.H., Shaknovich, R., Song, Z., Lu, P., Pandey, A., Melnick, A.M., Sinha, U., and Wang, Y.L. (2011). SYK inhibition and response prediction in diffuse large B-cell lymphoma. Blood *118*, 6342–6352.

Cho, K.R., and Shih, IeM. (2009). Ovarian cancer. Annu. Rev. Pathol. *4*, 287–313.

Coopman, P.J., Do, M.T., Barth, M., Bowden, E.T., Hayes, A.J., Basyuk, E., Blancato, J.K., Vezza, P.R., McLeskey, S.W., Mangeat, P.H., and Mueller, S.C. (2000). The Syk tyrosine kinase suppresses malignant growth of human breast cancer cells. Nature *406*, 742–747.

Couture, C., Songyang, Z., Jascur, T., Williams, S., Tailor, P., Cantley, L.C., and Mustelin, T. (1996). Regulation of the Lck SH2 domain by tyrosine phosphorylation. J. Biol. Chem. *271*, 24880–24884.

Currie, K.S., Kropf, J.E., Lee, T., Blomgren, P., Xu, J., Zhao, Z., Gallion, S., Whitney, J.A., Maclin, D., Lansdon, E.B., et al. (2014). Discovery of GS-9973, a selective and orally efficacious inhibitor of spleen tyrosine kinase. J. Med. Chem. *57*, 3856–3873.

Daniels, B.R., Perkins, E.M., Dobrowsky, T.M., Sun, S.X., and Wirtz, D. (2009). Asymmetric enrichment of PIE-1 in the Caenorhabditis elegans zygote mediated by binary counterdiffusion. J. Cell Biol. *184*, 473–479.

Faruki, S., Geahlen, R.L., and Asai, D.J. (2000). Syk-dependent phosphorylation of microtubules in activated B-lymphocytes. J. Cell Sci. *113*, 2557–2565.

Feldman, A.L., Sun, D.X., Law, M.E., Novak, A.J., Attygalle, A.D., Thorland, E.C., Fink, S.R., Vrana, J.A., Caron, B.L., Morice, W.G., et al. (2008). Overexpression of Syk tyrosine kinase in peripheral T-cell lymphomas. Leukemia *22*, 1139–1143.

Friedberg, J.W., Sharman, J., Sweetenham, J., Johnston, P.B., Vose, J.M., Lacasce, A., Schaefer-Cutillo, J., De Vos, S., Sinha, R., Leonard, J.P., et al. (2010). Inhibition of Syk with fostamatinib disodium has significant clinical activity in non-Hodgkin lymphoma and chronic lymphocytic leukemia. Blood *115*, 2578–2585.

Geahlen, R.L. (2014). Getting Syk: spleen tyrosine kinase as a therapeutic target. Trends Pharmacol. Sci. *35*, 414–422.

Gioia, R., Leroy, C., Drullion, C., Lagarde, V., Etienne, G., Dulucq, S., Lippert, E., Roche, S., Mahon, F.X., and Pasquet, J.M. (2011). Quantitative phosphoproteomics revealed interplay between Syk and Lyn in the resistance to nilotinib in chronic myeloid leukemia cells. Blood *118*, 2211–2221.

Goold, R.G., Owen, R., and Gordon-Weeks, P.R. (1999). Glycogen synthase kinase 3beta phosphorylation of microtubule-associated protein 1B regulates the stability of microtubules in growth cones. J. Cell Sci. *112*, 3373–3384.

Gundersen, G.G., Kalnoski, M.H., and Bulinski, J.C. (1984). Distinct populations of microtubules: tyrosinated and nontyrosinated alpha tubulin are distributed differently in vivo. Cell *38*, 779–789.

Hoellenriegel, J., Coffey, G.P., Sinha, U., Pandey, A., Sivina, M., Ferrajoli, A., Ravandi, F., Wierda, W.G., O'Brien, S., Keating, M.J., and Burger, J.A. (2012). Selective, novel spleen tyrosine kinase (Syk) inhibitors suppress chronic lymphocytic leukemia B-cell activation and migration. Leukemia *26*, 1576–1583.

Holgado-Madruga, M., and Wong, A.J. (2003). Gab1 is an integrator of cell death versus cell survival signals in oxidative stress. Mol. Cell. Biol. *23*, 4471–4484.

Holohan, C., Van Schaeybroeck, S., Longley, D.B., and Johnston, P.G. (2013). Cancer drug resistance: an evolving paradigm. Nat. Rev. Cancer *13*, 714–726.

Hutchcroft, J.E., Harrison, M.L., and Geahlen, R.L. (1991). B lymphocyte activation is accompanied by phosphorylation of a 72-kDa protein-tyrosine kinase. J. Biol. Chem. *266*, 14846–14849.

Jinawath, N., Vasoontara, C., Yap, K.L., Thiaville, M.M., Nakayama, K., Wang, T.L., and Shih, I.M. (2009). NAC-1, a potential stem cell pluripotency factor, contributes to paclitaxel resistance in ovarian cancer through inactivating Gadd45 pathway. Oncogene *28*, 1941–1948.

Jinawath, N., Vasoontara, C., Jinawath, A., Fang, X., Zhao, K., Yap, K.L., Guo, T., Lee, C.S., Wang, W., Balgley, B.M., et al. (2010). Oncoproteomic analysis reveals co-upregulation of RELA and STAT5 in carboplatin resistant ovarian carcinoma. PLoS ONE *5*, e11198.

Keshvara, L.M., Isaacson, C., Harrison, M.L., and Geahlen, R.L. (1997). Syk activation and dissociation from the B-cell antigen receptor is mediated by phosphorylation of tyrosine 130. J. Biol. Chem. *272*, 10377–10381.

Koti, M., Gooding, R.J., Nuin, P., Haslehurst, A., Crane, C., Weberpals, J., Childs, T., Bryson, P., Dharsee, M., Evans, K., et al. (2013). Identification of the IGF1/PI3K/NF κB/ERK gene signalling networks associated with chemotherapy resistance and treatment response in high-grade serous epithelial ovarian cancer. BMC Cancer *13*, 549.

Krisenko, M.O., Cartagena, A., Raman, A., and Geahlen, R.L. (2014). Nanomechanical property maps of breast cancer cells as determined by multiharmonic atomic force microscopy reveal Syk-dependent changes in microtubule stability mediated by MAP1B. Biochemistry *54*, 60–68.

L'Hernault, S.W., and Rosenbaum, J.L. (1985). Reversal of the posttranslational modification on Chlamydomonas flagellar alpha-tubulin occurs during flagellar resorption. J. Cell Biol. *100*, 457–462.

Law, C.L., Chandran, K.A., Sidorenko, S.P., and Clark, E.A. (1996). Phospholipase C-gamma1 interacts with conserved phosphotyrosyl residues

in the linker region of Syk and is a substrate for Syk. Mol. Cell. Biol. *16*, 1305–1315.

Lin, Y.H., Chen, B.Y., Lai, W.T., Wu, S.F., Guh, J.H., Cheng, A.L., and Hsu, L.C. (2015). The Akt inhibitor MK-2206 enhances the cytotoxicity of paclitaxel (Taxol) and cisplatin in ovarian cancer cells. Naunyn Schmiedebergs Arch. Pharmacol. *388*, 19–31.

Liu, Y.M., Chen, H.L., Lee, H.Y., and Liou, J.P. (2014). Tubulin inhibitors: a patent review. Expert Opin Ther Pat *24*, 69–88.

Luangdilok, S., Box, C., Patterson, L., Court, W., Harrington, K., Pitkin, L., Rhŷs-Evans, P., O-charoenrat, P., and Eccles, S. (2007). Syk tyrosine kinase is linked to cell motility and progression in squamous cell carcinomas of the head and neck. Cancer Res. *67*, 7907–7916.

Mócsai, A., Ruland, J., and Tybulewicz, V.L. (2010). The SYK tyrosine kinase: a crucial player in diverse biological functions. Nat. Rev. Immunol. *10*, 387–402.

Nakashima, H., Natsugoe, S., Ishigami, S., Okumura, H., Matsumoto, M., Hokita, S., and Aikou, T. (2006). Clinical significance of nuclear expression of spleen tyrosine kinase (Syk) in gastric cancer. Cancer Lett. *236*, 89–94.

Ong, S.E., Blagoev, B., Kratchmarova, I., Kristensen, D.B., Steen, H., Pandey, A., and Mann, M. (2002). Stable isotope labeling by amino acids in cell culture, SILAC, as a simple and accurate approach to expression proteomics. Mol. Cell. Proteomics *1*, 376–386.

Peters, J.D., Furlong, M.T., Asai, D.J., Harrison, M.L., and Geahlen, R.L. (1996). Syk, activated by cross-linking the B-cell antigen receptor, localizes to the cytosol where it interacts with and phosphorylates alpha-tubulin on tyrosine. J. Biol. Chem. *271*, 4755–4762.

Piperno, G., and Fuller, M.T. (1985). Monoclonal antibodies specific for an acetylated form of alpha-tubulin recognize the antigen in cilia and flagella from a variety of organisms. J. Cell Biol. *101*, 2085–2094.

Podolanczuk, A., Lazarus, A.H., Crow, A.R., Grossbard, E., and Bussel, J.B. (2009). Of mice and men: an open-label pilot study for treatment of immune thrombocytopenic purpura by an inhibitor of Syk. Blood *113*, 3154–3160.

Ruzza, P., Biondi, B., and Calderan, A. (2009). Therapeutic prospect of Syk inhibitors. Expert Opin Ther Pat *19*, 1361–1376.

Thompson, W.C. (1977). Post-translational addition of tyrosine to alpha tubulin in vivo in intact brain and in myogenic cells in culture. FEBS Lett. *80*, 9–13.

Trivedi, N., Marsh, P., Goold, R.G., Wood-Kaczmar, A., and Gordon-Weeks, P.R. (2005). Glycogen synthase kinase-3beta phosphorylation of MAP1B at Ser1260 and Thr1265 is spatially restricted to growing axons. J. Cell Sci. *118*, 993–1005.

Uckun, F.M., Ek, R.O., Jan, S.T., Chen, C.L., and Qazi, S. (2010a). Targeting SYK kinase-dependent anti-apoptotic resistance pathway in B-lineage acute lymphoblastic leukaemia (ALL) cells with a potent SYK inhibitory pentapeptide mimic. Br. J. Haematol. *149*, 508–517.

Uckun, F.M., Qazi, S., Ma, H., Tuel-Ahlgren, L., and Ozer, Z. (2010b). STAT3 is a substrate of SYK tyrosine kinase in B-lineage leukemia/lymphoma cells exposed to oxidative stress. Proc. Natl. Acad. Sci. USA *107*, 2902–2907.

Vogelstein, B., Papadopoulos, N., Velculescu, V.E., Zhou, S., Diaz, L.A., Jr., and Kinzler, K.W. (2013). Cancer genome landscapes. Science *339*, 1546–1558.

Wang, W.H., Childress, M.O., and Geahlen, R.L. (2014). Syk interacts with and phosphorylates nucleolin to stabilize Bcl-x(L) mRNA and promote cell survival. Mol. Cell. Biol. *34*, 3788–3799.

Weinblatt, M.E., Kavanaugh, A., Burgos-Vargas, R., Dikranian, A.H., Medrano-Ramirez, G., Morales-Torres, J.L., Murphy, F.T., Musser, T.K., Straniero, N., Vicente-Gonzales, A.V., and Grossbard, E. (2008). Treatment of rheumatoid arthritis with a Syk kinase inhibitor: a twelve-week, randomized, placebo-controlled trial. Arthritis Rheum. *58*, 3309–3318.

Weinblatt, M.E., Kavanaugh, A., Genovese, M.C., Musser, T.K., Grossbard, E.B., and Magilavy, D.B. (2010). An oral spleen tyrosine kinase (Syk) inhibitor for rheumatoid arthritis. N. Engl. J. Med. *363*, 1303–1312.

Xue, L., Wang, W.H., Iliuk, A., Hu, L., Galan, J.A., Yu, S., Hans, M., Geahlen, R.L., and Tao, W.A. (2012). Sensitive kinase assay linked with phosphoproteomics for identifying direct kinase substrates. Proc. Natl. Acad. Sci. USA *109*, 5615–5620.

Xue, L., Geahlen, R.L., and Tao, W.A. (2013). Identification of direct tyrosine kinase substrates based on protein kinase assay-linked phosphoproteomics. Mol Cell Proteomics *12*, 2969–2980.

Zioncheck, T.F., Harrison, M.L., and Geahlen, R.L. (1986). Purification and characterization of a protein-tyrosine kinase from bovine thymus. J. Biol. Chem. *261*, 15637–15643.

Zioncheck, T.F., Harrison, M.L., Isaacson, C.C., and Geahlen, R.L. (1988). Generation of an active protein-tyrosine kinase from lymphocytes by proteolysis. J. Biol. Chem. *263*, 19195–19202.